Further Refining and Validation of RF Absorber Approximation Equations for Anechoic Chamber Predictions

Vince Rodriguez,
NSI-MI Technologies, Suwanee, Georgia, USA, vrodriguez@nsi-mi.com

***Abstract*—Indoor antenna ranges must have walls, floor and ceiling treated with RF absorber. The normal incidence performance of the absorber is usually provided by the manufacturers of the materials; however, the bi-static or off angle performance must also be known. In a recent paper [1], a polynomial approximation was introduced that gave a prediction of the reflected energy from pyramidal absorber. In this paper, the approximations are used to predict the quiet zone (QZ) performance of several anechoic chambers. These predictions are compared with measurements performed per the free space VSWR method of four different chambers. Among the chambers analyzed are a 7.3m by 3.65m by 3.65m range with a 24-inch absorber, operating from 1 to 6 GHz with a 91 cm spherical QZ and a 5.18 m path length. Another chamber is 7 m long by 3.3 m wide with a 2.4 m height. 12-inch absorber is used to treat the internal surfaces and the QZ changes from 63 cm to 20 cm from 2 GHz to 18 GHz. The path length is 5.18m. While performing the comparison, changes are made to the calculations to further improve the predictions of the computations. A chamber previously analyzed is computed again after the changes to see whether there are improvements in the prediction. The results show that the polynomial approximations can be used to give a reasonably accurate and safe prediction of the QZ performance of anechoic chambers and improve some of the previous comparisons especially at lower frequencies where the ray tracing is not that accurate.**

***Index Terms*—antenna measurements, Anechoic Chambers.**

I. Introduction

Recently a set of polynomial equations and coefficients were developed to predict the bi-static reflectivity of RF pyramidal absorber [1]. Using these polynomials and a simple ray tracing approach, the ability of these equations to predict the performance of anechoic chamber was checked against other numerical approaches [2] and to actual measurements of the QZ of implemented chambers [3]. The measurements of the QZ levels are done per the free space VSWR methodology [4]. Descriptions of this method for evaluating QZ reflectivity levels can be found in [5]. Recently, this methodology has been challenged, since it is being used in cases where it does not apply, and it is dependent on the directivity of the probe antennas [6]. In this paper, four different anechoic range geometries are analyzed using the methods described in [2] and [3]. The results are compared to measurements, the differences are explained, and further changes to the ray tracing method are done to achieve a better prediction of the QZ reflectivity. In performing the comparison, more limitations of the free space VSWR technique are highlighted.

II. Simplified Ray-Tracing Approach

The simplified ray-tracing approach is intended for rectangular anechoic chambers. As it has been shown in [2], this approach is also valid for near-field ranges and compact ranges.

The necessary input parameters are the internal size of the anechoic chamber, length (L), width, (W) and height (H). The thickness of the absorber (t) used on the side walls, floor, ceiling and end wall are also required parameters. The size of the QZ and the distance from its center to the source antenna must be known (PL). Finally, the distance from the center of the QZ to the back wall must also be known (S). From these parameters, the angles of incidence onto the sidewalls, ceiling and floor can be computed. The angle of incidence θ and the absorber thickness t are the necessary input values for the absorber reflectivity equations introduced in [1].

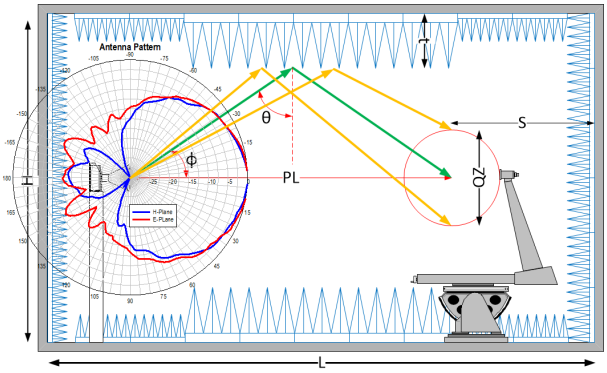

Figure 1. An Anechoic chamber geometry showing the different parameters. The width W is not shown but it will be analogous to the height H.

Figure 1 shows a typical anechoic chamber geometry and the different parameters required in the calculation. Simple geometry can be used to calculate the different angles of incidence for the top, center, and bottom of the QZ. The angle for the ray that is incident onto the center of the QZ (the green ray in Figure 1) is given by:

$$\theta = tan^{-1}\left(\frac{\frac{PL}{2}}{\frac{H}{2}-t}\right) \quad (1)$$

For the ray incident on to the top of the QZ, the angle of incidence is given by

$$\theta_{top} = tan^{-1}\left(\frac{PL}{H-2t-\frac{QZ}{2}}\right) \quad (2)$$

For the ray incident on the bottom of the QZ, as shown in figure 1, the angle of incidence is given by

$$\theta_{bottom} = tan^{-1}\left(\frac{PL}{H-2t+\frac{QZ}{2}}\right) \quad (3)$$

Using equation (1) provides a good average value for incidence, especially when the QZ is not extremely large compared to the path length (PL). A large QZ compare to PL occurs in anechoic chambers for near field measurements, in which case equations (2) and (3) may need to be considered.

Figure 1 illustrates the 3 factors that reduce the magnitude of the rays that reflect into the QZ from the side walls, ceiling, and floor. The first factor is the reflectivity of the absorber of thickness *t* at a given angle of incident (θ). This first factor is estimated from the Rodriguez Equations [1]. The second factor is the directivity of the range antenna. The ray incident onto the absorber at an angle θ leaves the antenna at an angle ϕ. There is a difference in level between the boresight radiation and the radiation in that ϕ direction. This range antenna pattern difference is given by $\Delta U = U(0) - U(\phi)$. The final factor is the additional path loss as the waves propagate. The difference between the reflected path and the direct path is given by $Loss = 20\log_{10}(RP/PL)$, where the RP is the reflected path length and PL is the path length as defined above. This is done for specular rays onto the lateral surfaces and the end wall behind the AUT, the QZ level is set as the higher of these reflectivity values.

III. Analysis and Comparison of Anechoic Ranges

A. Range 1: 7.01 m long by 3.35 m wide by 2.44 m high

To validate the ray-tracing approach using the Rodriguez Equations data was obtained for a series of antenna ranges that where measured using the free space VSWR technique. The first range studied is a rectangular anechoic chamber with an asymmetric (not square) cross-section. The QZ size is a 0.91 m diameter sphere, except for 2 GHz where a 0.63 m diameter sphere was measured. The path length or distance between the range antenna and the center of the QZ is 5.18 m. The Anechoic treatment is 0.305 m tall pyramidal absorber. The Range was measured and the results are shown in TABLE I.

TABLE I. Range 1 Measured Performance

Test Frequency (GHz)	*Range antenna directivity (dBi)*	*QZ size (m)*	*Measured reflectivity (dB)*
1	5	0.91	-11.7
2	15.5	0.63	-30.5
4	9.5	0.91	-36.1
10	11	0.91	-40.6
18	20	0.91	-50.68

The range antenna directivity is obtained from the technical specifications of the antennas used in the range during the free space VSWR test. The Range is analyzed using the methodology presented in [3]. The patterns for the range antennas are generated by using the higher level of the E and H plane at a given angle for the calculated pattern of a square aperture on a ground plane illuminated with a TE10 mode [7]. The directivity of such square aperture can be approximated using [7]:

$$D(dB) = 10 \cdot \log_{10}\frac{0.81 \cdot 4\pi \cdot a^2}{\lambda^2} \quad (4)$$

The size of the side of the square aperture (a) is chosen to provide the directivity of the actual range antennas. Figure 2 shows the estimated patterns used by the ray tracing geometrical optics method to calculate the reflectivity of the QZ. This is the same approach that was used in [3] when the actual patterns of the antennas are not available. The analysis using the (GO) and the Rodriguez's Polynomials introduced in [1] was performed. The results are presented in TABLE II.

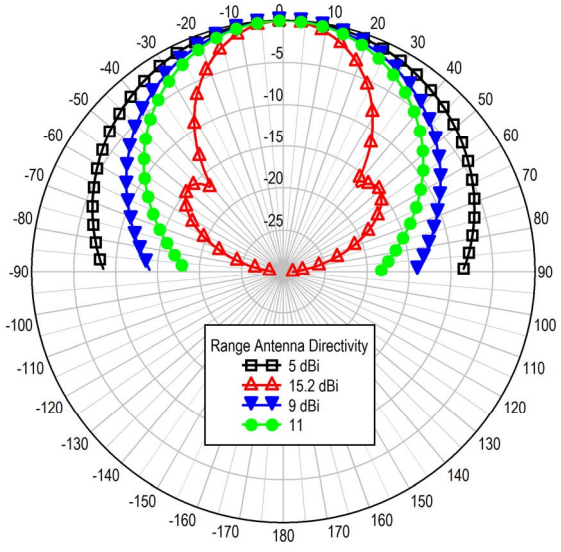

Figure 2. Approximated patterns for the range antennas for range 1.

TABLE II. RANGE 1 ANALYSIS AND MEASUREMENT

Freq. (GHz)	*Range antenna directivity (dBi)*	*QZ size (m)*	*Measured reflectivity (dB)*	*Calculated reflectivity (dB)*
1	5	0.91	-11.7	-6
2	15.5	0.63	-30.5	-15
4	9.5	0.91	-36.1	-17
10	11	0.91	-40.6	-46
18	20	0.91	-50.7	<-50

In this case, the comparison between measured and calculated reflectivity is not very good. Furthermore, unlike the first comparison in [3], the size of the QZ cannot be blamed as the cause for the difference. In reference [3], the QZ was 0.33λ at 100MHz; but in the present case, Range 1 has a QZ that is at least 3λ.

Figure 3 shows a traveling wave in the x direction at 100 MHz and at 1 GHz. The magnitude of that wave is 10 V/m. Two other waves 1 V/m in amplitude travel in the 45° and -45° direction. An interference pattern of standing waves is created. Figure 3 shows that it is possible to observe several standing waves at 1 GHz, while for 100 MHz, it was not possible to get an accurate VSWR to extract the reflectivity of the QZ.

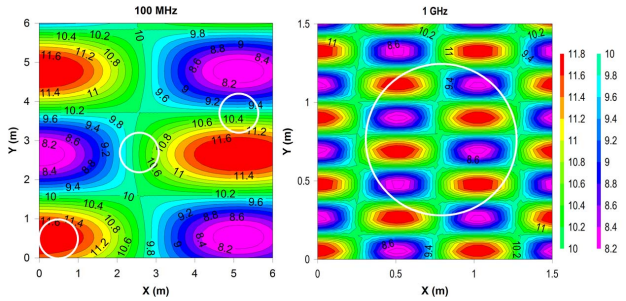

Figure 3. Simulated interference from reflections at 100 MHz and 1 GHz for a 1m Diameter QZ.

Hence, unlike in [3], the difference between the prediction and the measurement cannot be reconciled by looking at the potential of an electrically small QZ. Additionally, the large difference between predicted and measured reflectivity is observed at higher frequencies as well. The results presented in [2] had validated the simplified ray-tracing using the Rodriguez Equations against a commercially available computational electromagnetics package. Hence, an explanation for the difference between the measured and calculated performance is needed.

The free space VSWR technique scans the QZ in a horizontal plane. The assumption in the original work [4] is that the chamber is square in cross section. That is not the case here. Given the chamber geometry, the angle of incidence onto the side walls is 64.1°, while the angle of incidence onto the floor and the ceiling is 72.8°. For the 0.305m pyramidal absorber the reflectivity per the Rodriguez's Equations in [1] is given in the following table:

TABLE III. REFLECTIVITY CALCULATIONS

Freq. (GHz)	*Absorber in wavelengths*	*Reflectivity at 64.1° (dB)*	*Reflectivity at 72.8° (dB)*
1	1.02	-11.3	-6.4
2	2.03	-17.8	-11.5
4	4.06	-31.2	-16.2
10	10.15	<-50	-45.2
18	18	<-50	<-50

To better emulate the way the free space VSWR measurement was performed, the analysis using the ray-tracing technique presented in [2] and [3] was reapplied to Range 1, ignoring the ceiling and the floor. The results for the measurement and the new calculation are shown in TABLE IV. By ignoring the ceiling and the floor in the analysis, a closer correlation between measured and calculated reflectivity is achieved, which better describes the measurement technique used. Some of the differences can be attributed to the approximated patterns shown in Figure 2 versus the actual patterns for the antennas used in the measurement.

TABLE IV. RANGE 1 ANALYSIS AND MEASUREMENT (SIDE WALLS ONLY)

Freq. (GHz)	*Range antenna directivity (dBi)*	*QZ size (m)*	*Measured reflectivity (dB)*	*Calculated reflectivity (dB)*
1	5	0.91	-11.7	-10
2	15.5	0.63	-30.5	-23
4	9.5	0.91	-36.1	-31
10	11	0.91	-40.6	<-50
18	20	0.91	-50.7	<-50

B. Range 2: 7.32 m long by 3.66 m wide by 3.66 m high

The second range analyzed is a rectangular anechoic chamber with a symmetric (square) cross-section. The QZ size is a 0.91 m diameter sphere. The path length or distance between the range antenna and the center of the QZ is PL= 5.18 m. The anechoic treatment is t=0.61 m tall pyramidal absorber on all critical surfaces. The separation S to the back wall is 1.52 m. The measured data from the free space VSWR test is shown in TABLE V.

TABLE V. RANGE 2 MEASURED PERFORMANCE

Test Frequency (GHz)	*Range antenna directivity (dBi)*	*QZ size (m)*	*Measured reflectivity (dB)*
1.2	15.0	0.91	-33.7
1.3	15.5	0.91	-34.21
1.4	16.0	0.91	-33.0
1.8	17.6	0.91	-35.2

Test Frequency (GHz)	*Range antenna directivity (dBi)*	*QZ size (m)*	*Measured reflectivity (dB)*
6	20	0.91	-52.2

The range antenna directivities are taken from the manufacturer's datasheets. When these parameters are used with the ray-tracing approach, the predicted reflectivity can be calculated. Table VI shows the comparison.

TABLE VI. RANGE 2 ANALYSIS AND MEASUREMENT

Freq. (GHz)	*Range antenna directivity (dBi)*	*QZ size (m)*	*Measured reflectivity (dB)*	*Calculated reflectivity (dB)*
1.2	15.0	0.91	-33.7	-18
1.3	15.5	0.91	-34.21	-18
1.4	16.0	0.91	-33.0	-19
1.8	17.6	0.91	-35.2	-29
6	20	0.91	-52.2	<-50

As in the previous case, the predictions are extremely conservative. Unlike Range 1, the Range 2 results cannot be explained by the asymmetric chamber.

A different explanation is required. One possibility could be the approximated antenna patterns. A standard horn antenna is used from 1.2 to 1.8 GHz. The horn patterns computed using CST Suite™ from the antenna manufacturer's data sheet is shown in Figure 4.

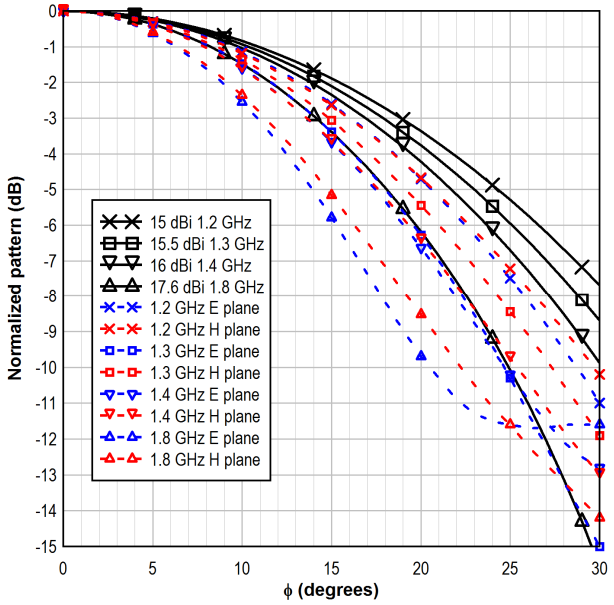

Figure 4. Patterns for a Seavey SGA-10 SGH used as source antenna compared to the approximated patterns used in the analysis.

The standard gain horn (SGH) used as the source has patterns for the E and H planes that are different from the calculated patterns from the square TE10 illuminated aperture on a ground plane. When comparing the SGH pattern to the approximations at ϕ=23.1°, where ϕ is the angle defined in Figure 1, are not enough to explain the differences between the prediction and the measurements. For 1.2 GHz the difference is 1.7 dB. At 1.4GHz the difference is 2.8 dB At 1.3 and 1.8 GHz the difference is 2.13 dB. There are some differences, but not enough to explain the differences shown in TABLE VI.

The other parameter is the angle of incidence. In general equation (1) is used to compute the angle of incidence. Hence, we take the tips of the absorber as the point at which the reflection occurs. If we assume that the reflection point is at the base of the absorber, that is, the wave penetrates the pyramids and it attenuates as it propagates into the absorber and the it is reflected by the metallic backing of the absorber to be reflected back into the range, after undergoing amplitude attenuation from the lossy material. Then equation (2) can be rewritten as

$$\theta_{top} = tan^{-1}\left(\frac{PL}{H-\frac{QZ}{2}}\right) \quad (5)$$

Using (5) in the calculation for the worst case reflectivity provides the following results:

TABLE VII. RANGE 2 ANALYSIS AND MEASUREMENT USING (5)

Freq. (GHz)	*Range antenna directivity (dBi)*	*QZ size (m)*	*Measured reflectivity (dB)*	*Calculated reflectivity (dB)*
1.2	15.0	0.91	-33.7	-35
1.3	15.5	0.91	-34.21	-38
1.4	16.0	0.91	-33.0	-41
1.8	17.6	0.91	-35.2	-49
6	20	0.91	-52.2	<-50

These calculated results are closer to those measured, but they seem too optimistic, and the goal of this approach using the equations in [1] is to provide a safe, conservative, prediction of the range requirements. If we choose the approximation of modeling the pyramidal absorber as a slab that is 1/3 the total pyramid height as described by Krauss [8], then (2) becomes

$$\theta_{top} = tan^{-1}\left(\frac{PL}{H-\frac{2}{3}t-\frac{QZ}{2}}\right) \quad (6)$$

And the analysis provides the results in Table VIII, which are closer to the measured results.

TABLE VIII. RANGE 2 ANALYSIS AND MEASUREMENT USING (6)

Freq. (GHz)	*Range antenna directivity (dBi)*	*QZ size (m)*	*Measured reflectivity (dB)*	*Calculated reflectivity (dB)*
1.2	15.0	0.91	-33.7	-30
1.3	15.5	0.91	-34.21	-32
1.4	16.0	0.91	-33.0	-35

Freq. (GHz)	*Range antenna directivity (dBi)*	*QZ size (m)*	*Measured reflectivity (dB)*	*Calculated reflectivity (dB)*
1.8	17.6	0.91	-35.2	-47
6	20	0.91	-52.2	<-50

This change to the way the reflected ray angle is computed provides a better result when the thickness of the absorber is less than 2.7λ. When the absorber is larger, for example 2.84, we can use (2). In TABLE VI, the values from the measurement were -35.2dB while the prediction was -29. If we subtract the 2.13dB difference from the patterns the reflectivity should be -31.13, so the difference is much smaller.

IV. REVISITING TWO PREVIOUS CASES

In [3], two cases were analyzed and compared to free space measurements. The first of the two cases was a large far field range. The anechoic chamber is 18 m long by 11.5 m wide and 11.5 m in height. The QZ is a 1 m diameter sphere. The path length is 12 m. All surfaces are treated with 1.82 m long pyramids except for the wall behind the source antenna, which is treated with 1.22 m long pyramids. The simulation provided a reflectivity of -11 dB compared to a measured level of -16.8 dB. Using equation (5), the result is -14 dB which is closer to the measured results.

The second case analyzed in [3] was a 6.1 m x 6.1 m x 13.4 1 m chamber. The chamber has a 1.98 m spherical QZ located at one end of the chamber. The chamber is lined with 91.4 cm absorber on the end wall behind the QZ and with 1.22 m absorber on the critical areas of the sidewalls, floor, and ceiling. The path length is 7.62 m. At 800MHz, the calculated reflectivity was -25 dB compared to -32.2 dB of the measurement. That computed value used (1) instead of (2). In that case, given the size of the QZ (1.98 m), attention should be paid to the other possible reflected rays entering the QZ. The angles of incidence for these rays are given by (2) and (3). Using (2) the computed reflectivity was -13 dB, almost 19dB difference. Using (6) to compute the angle of the reflected ray the new computed reflectivity is -29 dB which is much closer to the measured reflectivity.

V. CONCLUSION

The continuous comparison of the predicted performance using the Rodriguez's Equations [1] with measured results from implemented ranges using the free space VSWR technique has helped in improve the prediction approach. In addition, these comparisons also helped in identifying some of limitations of the free space VSWR technique. One of these limitations is that the QZ diameter should be large enough to cover at least one wavelength at the testing frequency to be able to pick up the ripple on the QZ scans [3]. Another limitation of the technique is that the anechoic range should be very close to square in cross section. As the analysis in range 1 showed, since the scanning is only conducted on the horizontal plane, only the reflectivity of the side walls is measured. These limitations of the technique in addition to the ones presented in [6] should be consider in future versions of the IEEE STD 149 [8]. Finally, the comparison has helped in getting a newer equation for the angle of incidence based on the frequency and the electrical thickness of the absorber that provides a more accurate prediction of the QZ reflectivity when compared to the free space VSWR measurements.

REFERENCES

[1] V. Rodriguez, E. Barry "A Polynomial Approximation for the Prediction of Reflected Energy from Pyramidal RF Absorbers" 38th annual Antenna Measurement Techniques Association Symposium AMTA 2016, Austin, TX, November 2016.

[2] V. Rodriguez "Validation of the Polynomial for RF Absorber Reflectivity for the Prediction of Anechoic Chambers" 2017 IEEE International Symposium on Antennas and Propagation and USNC/URSI National Radio Science Meeting, San Diego, California, July 9-14, 2017.

[3] V. Rodriguez, "Comparing Predicted Performance of Anechoic Chambers to Free Space VSWR Measurements," 39th Annual Meeting and Symposium of the Antenna Measurement Techniques Association AMTA 2017, Atlanta, GA, October 2017.

[4] University of Michigan Report 5391-1-F, February 1963.

[5] B. Tian "Free Space VSWR Method for Anechoic Chamber Electromagnetic Evaluation" Proceedeings of the 30th Annual Symposium of the Antenna Measurement Techniques Association (AMTA 2008), pp. 524–529, November 2008.

[6] Z Chen, Z. Xiong, and A. Enayati " Limitations of the Free Space VSWR Measurements for Chamber Validation" Proceedings of the 38th annual Symposium of the Antenna Measurement Techniques Association (AMTA 2016), pp. 144–148, October 2016.

[7] C. Balanis *Antenna Theory: Analysis and Design* 2nd Ed. Wiley, 1996

[8] J. D. Krauss *Antennas* 2nd ed. McGraw-Hill: Boston, Massachusetts, 1988 pp. 817-818

[9] *IEEE Standard Test Procedures for Antennas*, IEEE Standard 149-1979, 1979